Supporting Information

Li et al. 10.1073/pnas.1108840108

SI Materials and Methods.

RNA Extraction and cDNA Synthesis. Total RNA was extracted with the RNeasy Plant Mini Kit (Qiagen) from seven-day old whole seedlings grown on half-strength MS plates (1) or from leaves of 20-day old plants grown in soil. During extraction, in-column DNA digestions were conducted using RNase-free DNase Set (Qiagen) to remove possible genomic DNA contamination, according to manufacturer's description. The reverse transcriptions were performed using the SuperScript III First-Strand Synthesis System (Invitrogen) according to manufacturer's protocol. The single-stranded cDNA product (recovered in 20 μL) was diluted 10 times with water, and a 2-μL sample was used as the template for each PCR amplification in either the cloning of the double-stranded cDNA or in the transcription level analysis.

Isolation and Genotyping of Insertional Null Mutants. To isolate and screen for mutants that are homozygous for the insertional allele of interest, genomic PCR was performed with genomic DNA extracted from leaves (2) as the template, using Apex Taq RED DNA Polymerase Master Mix (Genesee Scientific).

The *atlpxa-1* transferred DNA (T-DNA) mutant was isolated from the collection available at the *Arabidopsis* knockout facility of the *Arabidopsis* Functional Genomics Center of the University of Wisconsin-Madison (3). PCR-based screening was conducted using the gene-specific primer pair DL26 and DL27 (Table S1). Three rounds of screening revealed the presence of an *AtLpxA* T-DNA insertion mutant in pool H175 (CSH175), and then in the subpool CSJ4349. The flanking sequence of the T-DNA insertion confirmed that the T-DNA was inserted in the fifth intron of *AtLpxA* (Fig. S1).

For genotyping purposes, the inserted DNA (T-DNA or transposon) was identified from a left border primer (LBa1 for the SALK lines, JL-202 for *atlpxa-1*, p745 for *atlpxd1-1*, or Ds33 for *atlpxd2-1*) (3–6) and a gene-specific primer (Table S1). The homozygous mutants were characterized by a second round of PCR analysis using gene-specific primer pairs flanking insertion sites. In this study, the following primer pairs were used (Table S1): JL-202/CJL001 and CJL001/CJL002 for *atlpxa-1*, LBa1/CJL061 and CJL060/CJL061 for *atlpxa-2*, LBa1/CJL063 and CJL062/CJL063 for *atlpxa-3*, p745/CJL083 and CJL082/CJL083 for *atlpxd1-1*, Ds33/CJL014 and CJL043/CJL014 for *atlpxd2-1*, LBa1/CJL085 and CJL017/CJL018 for *atlpxb-1* and *atlpxb-2*, LBa1/CJL019 and CJL019/CJL086 for *atlpxk-1*, LBa1/CJL089 and CJL088/CJL089 for *atlpxk-2*, LBa1/CJL091 and CJL090/CJL091 for *atlpxk-3*, and LBa1/CJL097 and CJL055/CJL097 for *atkdta-1*.

To characterize each of the null mutants in more detail, RT-PCR was conducted using the appropriate single-stranded cDNA as template and the *Actin2* gene as the internal control. Gene-specific primer pairs were as follows: ACT-F/ACT-R for *Actin2*, CJL002/CJL003 for *AtLpxA*, CJL158/CJL159 for *AtLpxC1.1/2.1/3.1/3.2/4/5.1*, CJL011/CJL012 for *AtLpxD1*, CJL014/CJL015 and CJL014/CJL044 for *AtLpxD2*, CJL131/CJL132 for *AtLpxB*, CJL020/CJL021 for *AtLpxK*, and CJL024/CJL025 for *AtKdtA*. The locations of these insertional mutations are shown in Fig. S1.

Plasmid Construction and Plant Transformation. To generate GFP fusion constructs, either full-length *AtLpx* cDNA without a stop codon or a partial 5′ terminal portion of the *AtLpx* coding region was amplified from the reverse transcription products using Phusion high-fidelity DNA polymerase (Finnzyme). The amplified DNA products were cloned to the pENTR/D-TOPO Vector (Invitrogen) and then recombined into pMDC83 in-fame with C-terminal GFP6 cDNA (7) using the LR Clonase II system (Invitrogen) through homologous recombination, according to the manufacturer's description. Gene-specific primers were used as follows: CJL002/CJL003 for *AtLpxA*, CJL008/CJL009 for *AtLpxC1.1*, CJL011/CJL176 for *AtLpxD1*, CJL015/CJL177 for *AtLpxD2*, CJL018/CJL163 for *AtLpxB*, and CJL021/CJL165 for *AtLpxK* (Table S1). To generate the *AtLpxC-RNAi* construct, the conserved region of *AtLpxC* cDNA was amplified using the primer pair CJL008/CJL009, cloned to the pENTR/D-TOPO Vector, and then recombined into pK7GWIWG2(II) (8). The *Arabidopsis* Columbia-0 (Col-0) ecotype was transformed with *Agrobacterium tumefaciens* strain GV3101, harboring the above binary plasmids, by the floral dip method (9). Transformants were selected on 0.8% agar plates containing half-strength MS medium and 1% sucrose, supplemented with either 50 mg/L hygromycin (pMDC constructs) or 50 mg/L kanamycin (RNAi construct).

Liquid Chromatography/Mass Spectrometry Detection of Lipid A Precursors in *Arabidopsis*. Normal phase liquid chromatography (LC) coupled with multiple reaction monitoring of the lipid A biosynthetic intermediates in *Arabidopsis* was performed using an Agilent 1200 Quaternary LC system interfaced to a 4,000 Q-Trap hybrid triple quadrupole linear ion-trap mass spectrometer, equipped with a Turbo V ion source (Applied Biosystems). An Ascentis Si HPLC column (5 μm, 25 cm × 2.1 mm) was used for normal phase liquid chromatography. The dried total lipids, extracted from 10-mg samples of each of the *Arabidopsis* lines, were dissolved in 1 mL chloroform, and a 10-μL portion was injected onto the normal phase column for either LC–electrospray ionization (ESI)/MS or LC–multiple reaction monitoring (MRM) analysis. Mobile phase A consisted of chloroform/methanol/aqueous ammonium hydroxide (800:195:5, vol/vol/vol), mobile phase B consisted of chloroform/methanol/water/aqueous ammonium hydroxide (600:340:50:5, vol/vol/vol/vol) and mobile phase C consisted of chloroform/methanol/water/aqueous ammonium hydroxide (450:450:95:5, vol/vol/vol/vol). The elution program consisted of the following: 100% mobile phase A was held isocratically for 2 min and then linearly increased to 100% mobile phase B over 14 min and held at 100% B for 11 min. The LC gradient was then changed to 100% mobile phase C over 3 min and held at 100% C for 3 min, and finally returned to 100% A over 0.5 min and held at 100% A for 5 min. The total LC flow rate was 300 μL/min. The postcolumn splitter diverted approximately 10% of the LC flow to the Turbo V ion source of the 4,000 Q-Trap mass spectrometer. MRM was performed in the negative ion mode with MS settings as follows: curtain gas (CUR) = 20 psi, ion source gas 1 (GS1) = 20 psi, ion source gas 2 (GS2) = 30 psi, ion spray voltage (IS) = −4,500 V, heater temperature (TEM) = 350 °C, interface heater = ON, declustering potential (DP) = −40 V, entrance potential (EP) = −10 V, collision cell exit potential (CXP) = −5 V. The MRM pairs for the various lipid A precursors are summarized in Fig. S3.

For LC–ESI/MS/MS, the same column elution conditions were employed, but the effluent was analyzed with a QSTAR XL quadrupole time-of-flight tandem mass spectrometer (Applied Biosystems) The postcolumn splitter diverted approximately 10% of the LC eluent to the ESI source. Mass spectra were acquired in the negative ion mode. The negative electrospray voltage was set at −4,500 V. Other MS settings were as follows: CUR = 25 psi, GS1 = 20 psi, DP = −55 V, FP = −100 V. Nitrogen was used as the collision gas for MS/MS experiments. Data acquisition and analysis were performed using the Analyst QS software.

1. Murashige T, Skoog F (1962) A revised medium for rapid growth and bioassay with tobacco tissue cultures. *Physiol Plant* 15:473–497.
2. Stewart CN, Jr., Via LE (1993) A rapid CTAB DNA isolation technique useful for RAPD fingerprinting and other PCR applications. *BioTechniques* 14:748–750.
3. Krysan PJ, Young JC, Sussman MR (1999) T-DNA as an insertional mutagen in *Arabidopsis*. *Plant Cell* 11:2283–2290.
4. Alonso JM, et al. (2003) Genome-wide insertional mutagenesis of *Arabidopsis thaliana*. *Science* 301:653–657.
5. Woody ST, Austin-Phillips S, Amasino RM, Krysan PJ (2007) The WiscDsLox T-DNA collection: An *Arabidopsis* community resource generated by using an improved high-throughput T-DNA sequencing pipeline. *J Plant Res* 120:157–165.
6. Martienssen RA (1998) Functional genomics: Probing plant gene function and expression with transposons. *Proc Natl Acad Sci USA* 95:2021–2026.
7. Curtis MD, Grossniklaus U (2003) A gateway cloning vector set for high-throughput functional analysis of genes in planta. *Plant Physiol* 133:462–469.
8. Karimi M, Depicker A, Hilson P (2007) Recombinational cloning with plant gateway vectors. *Plant Physiol* 145:1144–1154.
9. Clough SJ, Bent AF (1998) Floral dip: A simplified method for Agrobacterium-mediated transformation of *Arabidopsis thaliana*. *Plant J* 16:735–743.

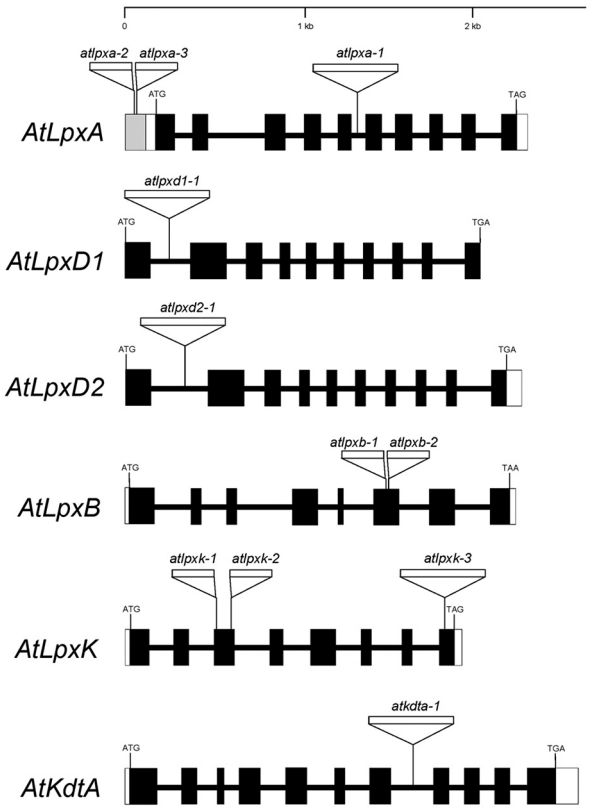

Fig. S1. Genome structures and schematic representation of the T-DNA or transposon insertions in the *Arabidopsis* lpx and kdtA genes. White boxes indicate 5′ or 3′ UTR of each gene. Exons are shown as black boxes. The spaces between each black box represent the introns. The *AtlpxA* promoter region is shown as a gray box.

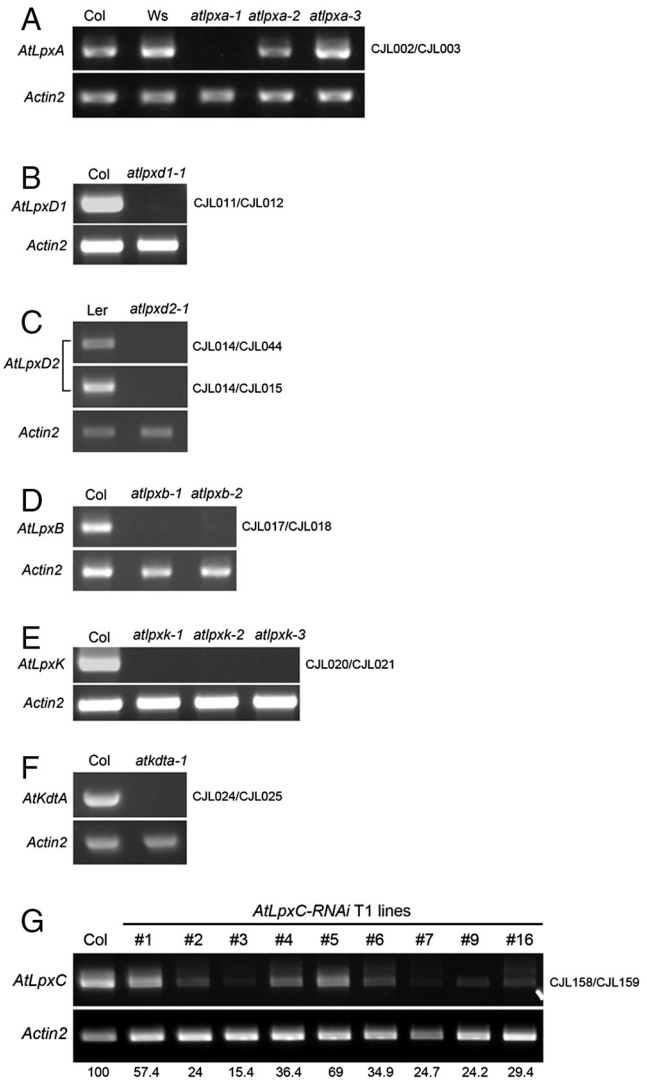

Fig. S2. Characterization of insertional mutants and RNAi transgenic lines used in this study by RT-PCR. (*A*–*F*) RT-PCR analysis of the *AtLpxA*, *AtLpxD1*, *AtLpxD2*, *AtLpxB*, *AtLpxK*, and *AtKdtA* genes in various *Arabidopsis* wild types and the corresponding mutants. The *atlpxa-1* mutation is the only null allele for *AtLpxA* among the three independent mutants analyzed in this study. Primer pairs used for each gene are shown on the right, and their sequences are listed in Table S1. (*G*) Analysis of *AtLpxC* expression in several *AtLpxC-RNAi* T1 generation plants. The primer pair (CJL158/CJL159) was chosen based on the regions of sequence identity common to the *AtLpxC1.1/2.1/3.1/3.2/4/5.1* cDNAs. Numbers below each lane (percent) show the relative expression level of *AtLpxC* mRNA normalized to that of the *Actin2* gene.

A

Lipid A Pathway Intermediates	Retention Time (min)	Precursor Ion	Product Ion	Substrate of	Product of
UDP-2,3-diacyl-GlcN	22	1016.5	385.0	LpxH, LpxB	LpxD
Lipid X	26	710.4	240.0	LpxB	LpxH
Disaccharide-1-P	23	1323.8	1097.7	LpxK	LpxB
Lipid IV_A	37	701.4	853.5	KdtA	LpxK
Reference Lipid					
PE (16:0/18:2)	17	714.5	279.2		

B

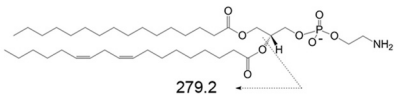

Phosphatidylethanolamine (PE, 16:0/18:2)
$[M-H]^-$ 714.5

C

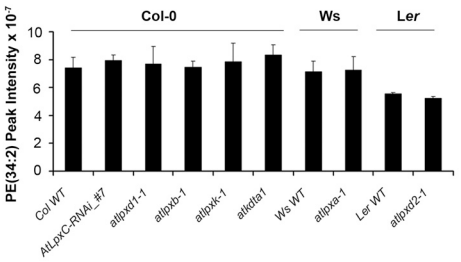

Fig. S3. Ion pairs used for detection by multiple reaction monitoring of lipid A pathway intermediates in *Arabidopsis*. (*A*) The indicated precursor/product ion pairs and retention times were used to identify the presence of lipid A pathway intermediates, having the structures shown in Fig. 1, in total plant lipids. All the negative precursor ions listed below are singly charged $[M-H]^-$ species, except for the precursor ion of lipid IV_A, which is observed as $[M-2H]^{2-}$. The product ions are all singly charged (proposed structures shown with each analysis below). (*B*) Structures of the parent (*m/z* 714.5) and predicted fragment ion (*m/z* 279.2) for the major species of endogenous phosphatidylethanolamine (16:0/18:2) present in *Arabidopsis* used as an internal reference against which the levels of the lipid A pathway intermediates were normalized. (*C*) Knockout mutants or RNAi transgenic plants show similar phosphatidylethanolamine (16:0/18:2) levels compared to wild type plants in the same ecotype background.

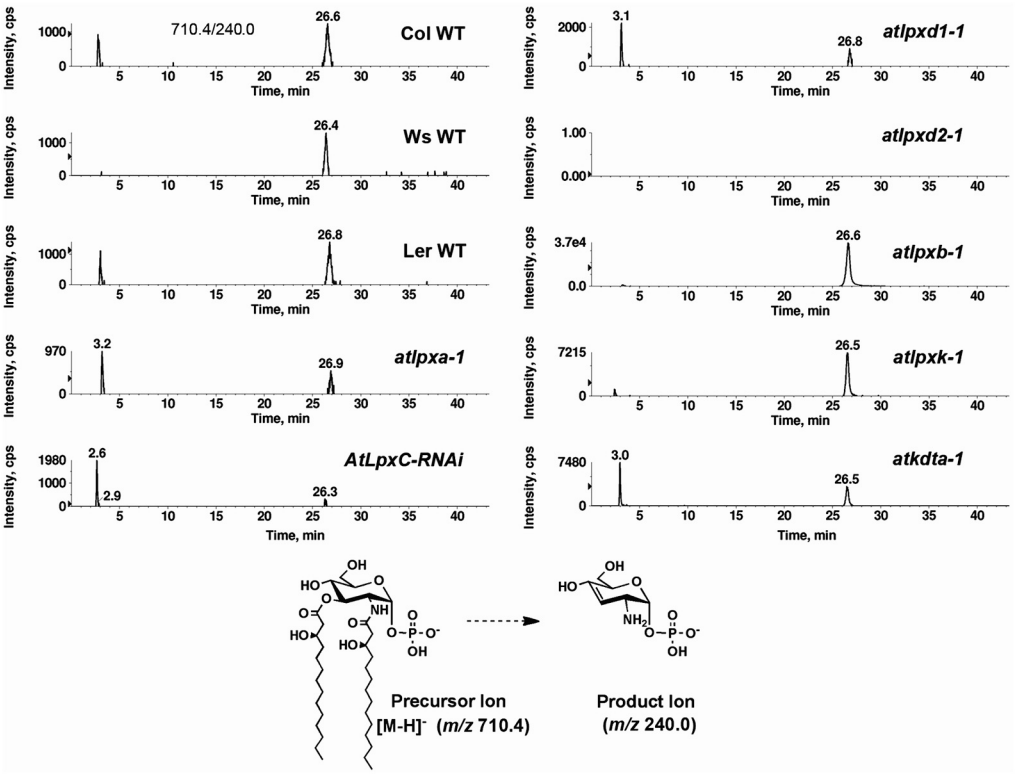

Fig. S4. LC–ESI/MRM analysis of lipid X in *Arabidopsis* wild type, mutants and transgenic RNAi plants. Lipid X, appearing at approximately 26 min, is detected in the total plant lipids using the MRM ion pair of 710.4/240.0 in the negative mode (proposed structures shown below). MRM detection using the alternative ion pair of 710.4/466.2 yields the same pattern (not shown).

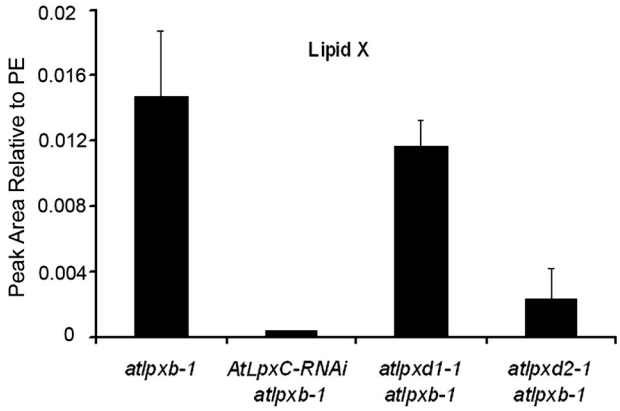

Fig. S5. Comparison of lipid X levels in *atlpxb-1*, *AtLpxC-RNAi/atlpxb-1*, *atlpxd1-1/atlpxb-1*, and *atlpxd2-1/atlpxb-1* plants.

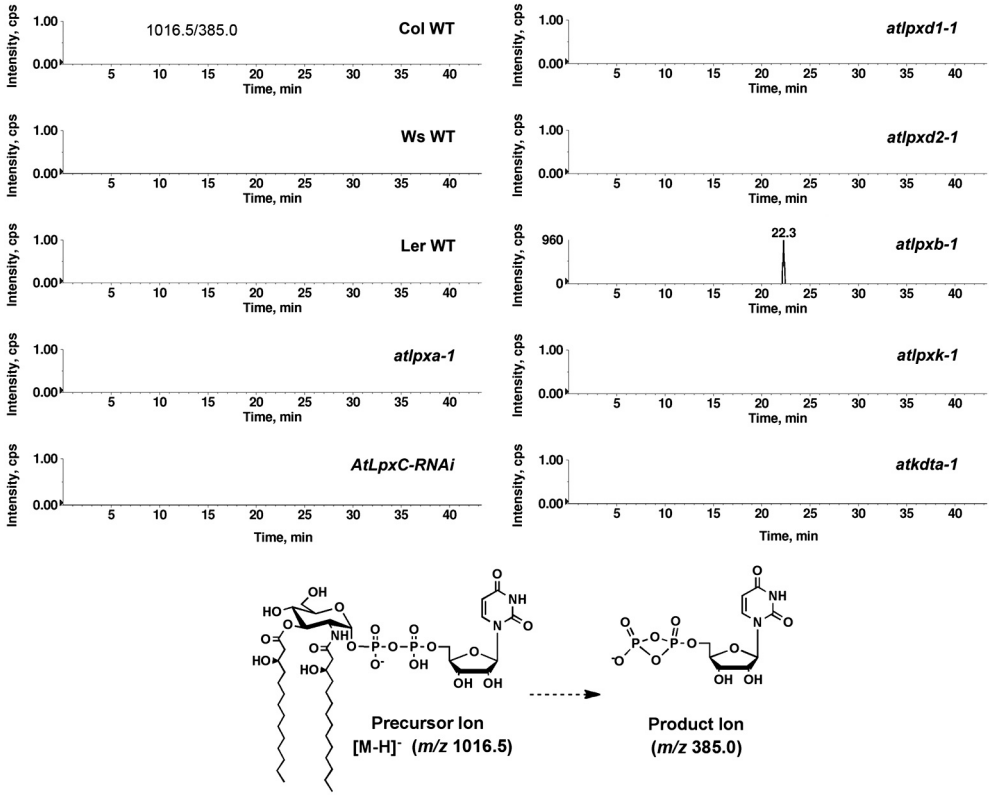

Fig. S6. LC–ESI/MRM analysis of UDP-2,3-diacylglucosamine in *Arabidopsis* wild type, mutants, and transgenic RNAi plants. UDP-2,3-diacylglucosamine, appearing at approximately 22 min, is detected in the total plant lipids using the MRM ion pair of 1,016.5/385.0 in the negative mode (proposed structures shown below). This compound is observed only in the *atlpxb-1* mutant lipids, in which it is expected to accumulate (Fig. 1). MRM detection using the alternative ion pair of 1,016.5/466.2 yields the same pattern (not shown).

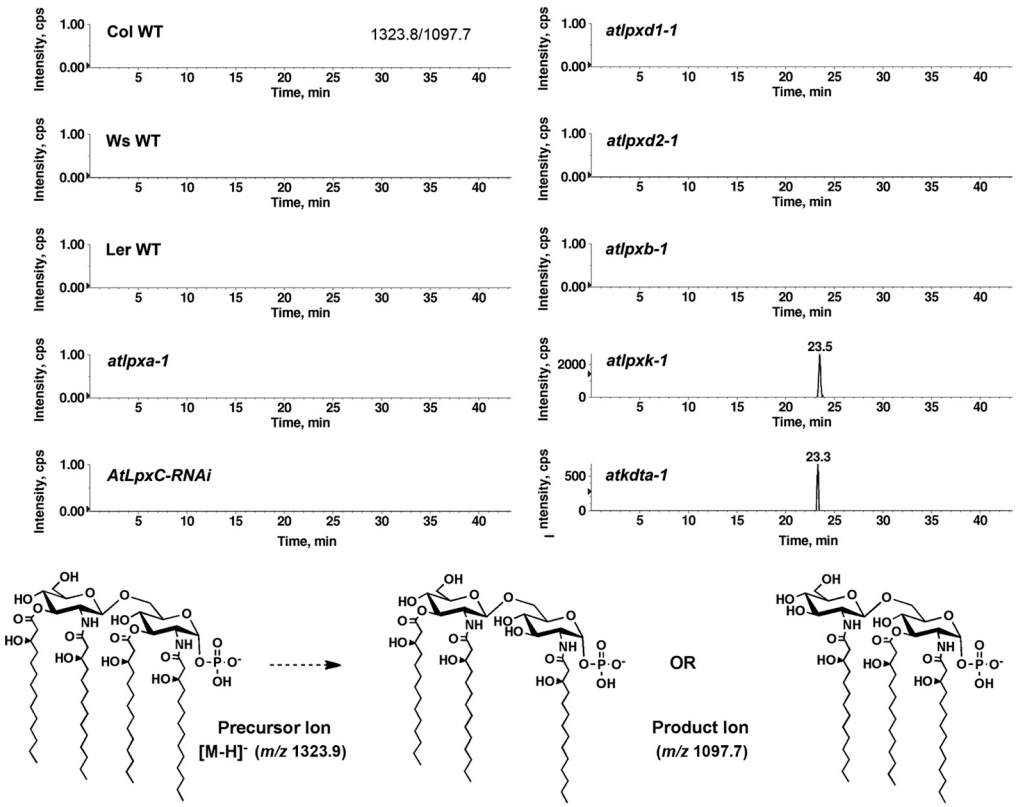

Fig. S7. LC–ESI/MRM analysis of the disaccharide 1-phosphate precursor in *Arabidopsis* wild type, mutants, and transgenic RNAi plants. The disaccharide 1-phosphate, appearing at approximately 23 min, is detected in the total plant lipids using the MRM ion pair of 1,323.8/1,097.7 in the negative mode (proposed structures shown below). This compound is observed only in the *atlpxk-1* and *atkdta-1* mutant lipids, in which it is expected to accumulate (Fig. 1). MRM detection using the alternative ion pair of 1,323.8/651.3 yields the same pattern (not shown).

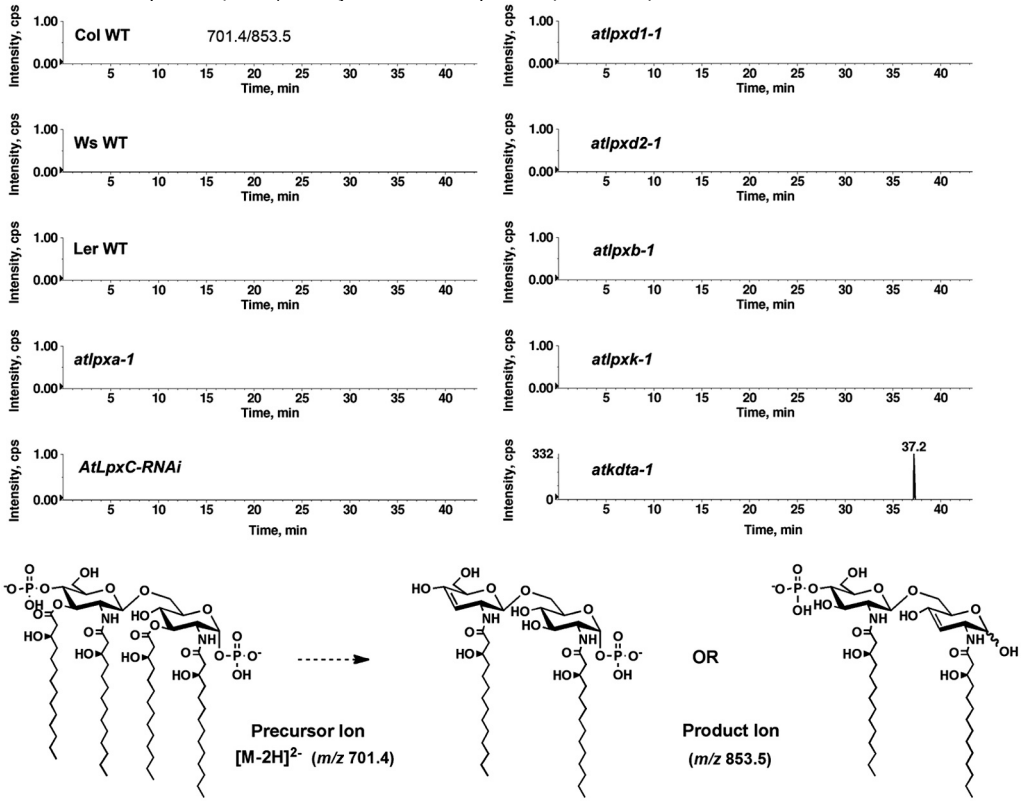

Fig. S8. LC–ESI/MRM analysis of the lipid IV_A precursor in Arabidopsis wild type, mutants, and transgenic RNAi plants. The lipid IV_A precursor, appearing at approximately 37 min, is detected in the total plant lipids using the MRM ion pair of 701.4/853.5 in the negative mode (proposed structures shown below). This compound is observed only in the *atkdta-1* mutant lipids, in which it is expected to accumulate (Fig. 1). MRM detection using the alternative ion pair of 1,403.8/1,097.7 yields the same pattern (not shown).

Table S1. Primers used in this work

Primer	Primer sequence	Primer	Primer sequence
ACT-F	TGGTGTCATGGTTGGGATG	CJL063	TGATGCCGAGAACGAATTATC
ACT-R	CACCACTGAGCACAATGTTAC	CJL082	AAGCGGTTTCAAGATTGTTTG
CJL001	CACCAGCGTTTAAACTCAAAAGCTAC	CJL083	ACCATCTTGACCAATGCAGAC
CJL002	AGTTGTGGAATCGAGCCATTGT	CJL085	AAGCAACGTTTGTTGGACATC
CJL003	CACCATGATTTCTCTCCTTAAAGCTC	CJL086	TGCTCTTGACAAATGCATCAG
CJL008	CACCATGAGACTCCCCGTCACCGT	CJL088	TTTGGCAGTGAAACAAATTGG
CJL009	GTCCATGGTAAGGTGACGTG	CJL089	TCAATTCCTCGTTGATTCTGG
CJL011	GTCTTCTTGAGTCTGGCAAACAGA	CJL090	TTTCTACTCCAAGATGGTGCC
CJL012	CACCATGGCAAATAGTTTGCGAAC	CJL091	GACATGTCTGCCTCACACATG
CJL014	GATTTCTCTCTTGTTCGCAATCTG	CJL097	GAGCGACACTGTACAATTCCC
CJL015	CACCATGGCGGCTACTCTTTGGAG	CJL131	GAGTTTTTGATTCTCTCTCTTCTC
CJL017	ACGCCTGGCATAACTAAGAATAGT	CJL132	AGTATCAAACAAAGGCATGTGA
CJL018	CACCATGATGTTTCAGATTACAAAGAGC	CJL158	CTAAGCCGTCGTTTCTCG
CJL019	CACCATGAGATCGATCTCACAAAGTT	CJL159	GTTTGATCGGTTAAAATGTCC
CJL020	ACTGGAAACATAGAACTTAGCAGC	CJL163	AATCACCGATTTAGCAGCT
CJL021	CACCATGGAGAAGCTGAGGAAGGT	CJL165	AGAGCGGCGGATTTGGA
CJL024	TTTGCATTCAATGTGATTTCT	CJL166	TAGGAAGGGAACGAGAGAAC
CJL025	CACCATGAAGCTCGGAGTGTTTGTA	CJL176	AGAGAAAAAACCTAGACCGCT
CJL043	AGTTTTAGACTTTACAGCCTGATG	DL26	TGATTTCTCTCCTTAAAGCTCGCGAGAAG
CJL044	GTGATTGGACCATCAGTTGACA	DL27	TAAGTTGTGGAATCGAGCCATTGTCTGAA
CJL055	GCCGCTTTTGACAAAACTATA	Ds33	TCGTTTCCGTCCCGCAAGT
CJL060	TTTGGGATTAGTTCCGAGTCC	JL-202	CATTTTATAATAACGCTGCGGACATCTAC
CJL061	ATCAAACCTTGCCAATCACAG	LBa1	TGGTTCACGTAGTGGGCCATCG
CJL062	TGCCTAGCTTCACTGAAGAGC	p745	AACGTCCGCAATGTGTTATTAAGTTGTC